BJP British Journal of Pharmacology

DOI:10.1111/bph.12684
www.brjpharmacol.org

RESEARCH PAPER

Cardiac responses to β-adrenoceptor stimulation is partly dependent on mitochondrial calcium uniporter activity

E Fernández-Sada[1]*, C Silva-Platas[1]*, C A Villegas[1], S L Rivero[1], B C Willis[1], N García[1,2], J R Garza[1], Y Oropeza-Almazán[1], C A Valverde[3], G Mazzocchi[3], C Zazueta[4], G Torre-Amione[1,2,5] and G García-Rivas[1,2]

[1]*Cátedra de Cardiología y Medicina Vascular, Escuela de Medicina, Tecnológico de Monterrey, Monterrey, Nuevo León, México,* [2]*Centro de Investigación Básica y Transferencia, Instituto de Cardiología y Medicina Vascular, Tec Salud, San Pedro Garza García, Nuevo León, México,* [3]*Centro de Investigaciones Cardiovasculares, Facultad de Ciencias Médicas, Universidad Nacional de La Plata, La Plata, Argentina,* [4]*Departamento de Biomedicina Cardiovascular, Instituto Nacional de Cardiología 'Ignacio Chávez', México City, D.F., México, and* [5]*Methodist DeBakey Heart and Vascular Center, The Methodist Hospital, Houston, TX, USA*

Correspondence
Dr Gerardo García-Rivas, Centro de Investigación Básica y Transferencia, Instituto de Cardiología y Medicina Vascular, Tec Salud, Batallón de San Patricio 112, Hospital Zambrano-Hellión, Edificio Escuela de Medicina, 2do, Nivel, San Pedro Garza García CP 66278, Nuevo León, México.
E-mail: gdejesus@itesm.mx

*These authors contributed equally to this work.

Received
23 July 2013
Revised
6 February 2014
Accepted
1 March 2014

BACKGROUND AND PURPOSE

Despite the importance of mitochondrial Ca^{2+} to metabolic regulation and cell physiology, little is known about the mechanisms that regulate Ca^{2+} entry into the mitochondria. Accordingly, we established a system to determine the role of the mitochondrial Ca^{2+} uniporter in an isolated heart model, at baseline and during increased workload following β-adrenoceptor stimulation.

EXPERIMENTAL APPROACH

Cardiac contractility, oxygen consumption and intracellular Ca^{2+} transients were measured in *ex vivo* perfused murine hearts. Ru_{360} and spermine were used to modify mitochondrial Ca^{2+} uniporter activity. Changes in mitochondrial Ca^{2+} content and energetic phosphate metabolite levels were determined.

KEY RESULTS

The addition of Ru_{360}, a selective inhibitor of the mitochondrial Ca^{2+} uniporter, induced progressively and sustained negative inotropic effects that were dose-dependent with an EC_{50} of 7 μM. Treatment with spermine, a uniporter agonist, showed a positive inotropic effect that was blocked by Ru_{360}. Inotropic stimulation with isoprenaline elevated oxygen consumption (2.7-fold), Ca^{2+}-dependent activation of pyruvate dehydrogenase (5-fold) and mitochondrial Ca^{2+} content (2.5-fold). However, in Ru_{360}-treated hearts, this parameter was attenuated. In addition, β-adrenoceptor stimulation in the presence of Ru_{360} did not affect intracellular Ca^{2+} handling, PKA or Ca^{2+}/calmodulin-dependent PK signalling.

CONCLUSIONS AND IMPLICATIONS

Inhibition of the mitochondrial Ca^{2+} uniporter decreases β-adrenoceptor response, uncoupling between workload and production of energetic metabolites. Our results support the hypothesis that the coupling of workload and energy supply is partly dependent on mitochondrial Ca^{2+} uniporter activity.

LINKED ARTICLES
This article is part of a recent themed issue on Mitochondrial Pharmacology: Energy, Injury & Beyond published in volume 171 issue 8. To view the other articles in this issue visit http://dx.doi.org/10.1111/bph.2014.171.issue-8

Abbreviations
$[Ca^{2+}]_m$, intramitochondrial calcium; CaMKII, Ca^{2+}/calmodulin-dependent PK; HR, heart rate; MCU, mitochondrial Ca^{2+} uniporter; MPi, mechanical performance index; MVO_2, myocardial oxygen consumption; LVP, left ventricular pressure; PCr, phosphocreatine; PDH, pyruvate dehydrogenase; PLB, phospholamban; PLFF, pulse local-field fluorescence; Spm, spermine; TBARS, thiobarbituric acid-reactive substances

Introduction

Cardiac excitation–contraction coupling consumes enormous amounts of cellular energy, which is mainly produced in mitochondria by oxidative phosphorylation. In order to support the constantly varying workload with energy supply, coordinated mechanisms are essential to maintain the availability of energetic phosphate metabolites (Maack and O'Rourke, 2007; Balaban, 2009). Intramitochondrial calcium ($[Ca^{2+}]_m$) has drawn attention as being a key player in the coupling of mitochondrial ATP production to cardiac workload. When a cardiac workload is imposed, the cytosolic-free calcium ($[Ca^{2+}]_c$) increases, which in turn results in $[Ca^{2+}]_m$ increase, an event that triggers activation of key dehydrogenases of the citric acid cycle, to match the production of NADH to its oxidation by the electron transport chain (McCormack *et al.*, 1990). This series of events is essential for a proper regulation of energy production and cardiac contractility. A critical step in this process is the uptake of Ca^{2+} from the cytosol into the mitochondria and neither the mechanisms nor the regulators that control this process are fully defined. Cytosolic Ca^{2+} influx into the mitochondrial matrix is mediated primarily by the highly selective calcium channel, mitochondrial Ca^{2+} uniporter (MCU) (Gunter and Pfeiffer, 1990). Functional and comparative genomics has led to the characterization of the MCU complex, which includes the channel-forming subunit MCU (Baughman *et al.*, 2011; De Stefani *et al.*, 2011) and its regulators MICU1, MICU2, MCUb, EMRE and MCUR1 (Perocchi *et al.*, 2010; Mallilankaraman *et al.*, 2012; Raffaello *et al.*, 2013; Sancak *et al.*, 2013), which are crucial for Ca^{2+} uptake.

While it is clear that this cluster of proteins has the capacity of transporting Ca^{2+} from the cytosol into the mitochondria in a large number of cell types, whether they play a role in normal cardiac cells is not known. In fact, because of the high speed of systolic Ca^{2+} transients in heart cells, the role of the MCU as a key regulator of the entry of Ca^{2+} into the mitochondria on a beat-to-beat mechanism remains a matter for debate (O'Rourke and Blatter, 2009).

But a series of observations from our group are in support of the central role of the MCU as a regulator of cardiac physiology and are germane to this discussion. First, in a model of cardiac ischaemia-reperfusion injury, treatment with Ru_{360}, a selective inhibitor of the MCU, prevented mitochondrial Ca^{2+} overload (García-Rivas *et al.*, 2006). Second, isolated mitochondria obtained from Ru_{360}-treated hearts decreased $[Ca^{2+}]_m$ (García-Rivas *et al.*, 2005) and, finally, Ru_{360}-treated hearts following ischaemia-reperfusion injury were less prone to undergo mitochondria permeability transition and apoptosis (García-Rivas *et al.*, 2006; Correa *et al.*, 2007). Taking these observations together suggests that the MCU plays a critical role in intramitochondrial Ca^{2+} handling at least in pathological conditions. However, the role of MCU under conditions of normal or physiological increases in contractility is not known. Accordingly, we set up a series of experiments with rat isolated hearts to determine the regulatory role of the MCU under unstimulated conditions of heart contractility and following β-adrenoceptor stimulation, assuming that an increase in $[Ca^{2+}]_m$ is essential for increasing ATP supply. Here, we identified that MCU inhibition results in a lower response to β-adrenoceptor stimulation and uncoupling of workload and myocardial oxygen consumption (MVO_2). We conclude that coupling of the workload to the energy supply was partly dependent on MCU activity.

Methods

Animals

All animal care and experimental procedures were in accordance with the animal care guidelines of the Guide for the Care and Use of Laboratory Animals published by the US National Institutes of Health and approved by the animal use and care committees of the School of Medicine of the Tecnológico de Monterrey (Project Nos. 2009-R006 and F2011-009) and La Plata University. All studies involving animals are reported in accordance with the ARRIVE guidelines for reporting experiments involving animals (Kilkenny *et al.*, 2010; McGrath *et al.*, 2010). A total of 67 rats and 10 mice were used in the experiments described here. Male Wistar rats (250–300 g) were obtained from the Tecnológico de Monterrey campus Animal Facility. Mice (17–28 g) were obtained from the La Plata Medical School animal facility. Animals were allowed free access to food and water and maintained on a 12-h light/dark cycle, with controlled temperature (22.5 ± 2°C) and humidity (45 ± 5%).

Rat isolated perfused hearts

The hearts were mounted in accordance with the Langendorff model and perfused at constant flow (12 $mL \cdot min^{-1}$) with Krebs–Henseleit (K-H) buffer that consisted of (in mM): 3.5 KCl, 116 NaCl, 26 $NaHCO_3$, 1.6 NaH_2PO_4, 0.7 $MgSO_4$, 1.5 $CaCl_2$, 11 glucose and 0.2 octanoate. The buffer was gassed

with 95% O_2-5% CO_2 and equilibrated at pH 7.4, 37°C (García-Rivas *et al.*, 2005). The pulmonary artery was cannulated and connected to a closed chamber to measure MVO_2 in the coronary effluent with a Clark-type oxygen electrode (Yellow Spring Instruments, Yellow Spring, OH, USA). The rate of MVO_2 was calculated as the difference between the concentration in the K-H buffer before (100%) and after perfusion. To obtain an isovolumetrically beating preparation, a latex balloon filled with water and connected by a catheter transducer was used (FOBS-28; WPI, Sarasota, FL, USA). Before each experimental protocol was initiated, the isolated hearts were set at a mean left ventricular pressure (LVP) of 60 ± 10 mmHg and were allowed to stabilize and wash out the potential residual catecholamines for 10–15 min. Heart rate (HR), LVP, mechanical performance index (MPi) (HR*LVP), and maximum positive and negative derivatives of LVP (±dP/dt) and MVO_2 were continuously recorded with Data Trax software (WPI). At the end of protocols, the atrial or ventricular tissue was removed from the perfusion system and immediately flash-frozen with liquid N_2, weighed and stored at –80°C.

Isolation of cardiomyocytes

Hearts were removed and mounted on the Langendorff apparatus as described above, and then perfused with collagenase-containing solution (1 mg·mL^{-1} collagenase type II; Worthington, Lakewood, NJ, USA) at 37°C as previously described (MacDonnell *et al.*, 2008). After enzymic treatment, the ventricles were dissected and mechanically disaggregated. Dissociated cells were filtered and rinsed in modified Tyrode buffer (composition in mM: 5.4 KCl, 128 NaCl, 0.4 NaH_2PO_4, 0.5 $MgCl_2$, 25 HEPES, 1.8 $CaCl_2$, 6 glucose, 5 creatine and 5 taurine, pH. 7.4 equilibrated with 100% O_2.

Measurement of mitochondrial Ca^{2+}

Frozen cardiac tissue from each experimental group was used to determine fractional activation of the pyruvate dehydrogenase (PDHa) (PDHa/PDHTotal) [E.C.1.2.4.1] as an indicator of $[Ca^{2+}]_m$, according to previous publications (Pepe *et al.*, 1999). We assessed PDH activity under extraction buffers in which both PDH phosphatase and PDH kinase were inhibited by KH_2PO_4, NaF, dichloroacetic acid and ADP. PDH activity was assessed spectrophotometrically following NADH production at 340 nm and 30°C (Pepe *et al.*, 1999). Mitochondria were prepared from isolated hearts by a rapid isolation method that was designed to minimize Ca^{2+} redistribution. At the end of each protocol, the heart was perfused with an ice-cold buffer containing (in mM) 250 sucrose, 1 EGTA, 0.001 diltiazem, 0.002 Ru_{360}, 0.002 cyclosporine A and 10 HEPES, pH 7.4, and was homogenized with a Polytron. $[Ca^{2+}]_m$ was measured by using the fluorescent indicator, Fluo-3 AM, assuming a dissociation constant, K_D = 310 nM, as described previously (García-Rivas *et al.*, 2005).

Measurement of Ca^{2+} transients

Ventricular cells were incubated for 30 min in Tyrode solution containing Fluo-3 AM (5 μM) and afterwards washed with a fluorophore-free solution. Fluorescent measurements were acquired with a Leica TCS SP5 confocal microscope, equipped with a D-156 apochromatic X63, 1.2 NA, oil objective. An argon laser was used to excite the fluorophore at 488 nm and emission collected at 500–600 nm. Line scan images were recorded along the longitudinal axis of the cell at 500 Hz. For Ca^{2+} transients, cells were field stimulated at 1 Hz. Fluorescence data were normalized as F/F_0, where F is fluorescence intensity and F_0 is average fluorescence at rest (MacDonnell *et al.*, 2008).

Perfused isolated hearts from mice were prepared according to Valverde *et al.* (2006). Rhod-2 (Invitrogen, Carlsbad, CA, USA) was used to evaluate intracellular calcium in the epicardial layer of the isolated hearts from mice using a custom-made setup for pulse local-field fluorescence (PLFF) microscopy. After dye loading and stabilization, hearts were paced at 5 Hz and perfused with Tyrode solution, as previously reported (Valverde *et al.*, 2006) with 0.5, 1 and 2 mM Ca^{2+} in the absence or presence of Ru_{360}. Ratio between emitted (F–F_0) and basal (F_0) fluorescence ($\Delta F/F_0$) was compared with 2 mM Ca^{2+} transient amplitude.

Quantification of energetic phosphate metabolites

Rat heart samples fast-frozen in liquid nitrogen were extracted by homogenizing in ice-cold 40% perchloric acid containing 0.5 mM EGTA. After 10 min on ice, the acid extract was centrifuged at 10 000× *g* for 2 min, and an aliquot of the supernatant was neutralized with KOH to pH 6.8. Within 1 h of extraction, the sample was thawed and used for HPLC separation and determination of energetic phosphate metabolites. After chromatographic separation, the peak area of each nucleotide in the chromatogram of the sample without added reference standards was subtracted from the corresponding peak area in the chromatogram of the sample with added standard nucleotides. Under these conditions the recovery of reference nucleotides and bases ranged from 90%. Nucleotide analyses were carried out with a dual-pump gradient HPLC system (Waters Chromatography, Toronto, Canada) as previously described (Ally and Park, 1992). Standard solutions were prepared in 0.1 M KH_2PO_4, pH 7.0, and stored at –80°C to minimize the degradation of phosphocreatine (PCr). The standard curves were subjected to linear regression analysis and calibration factors were determined.

Measurement of oxidative stress and GSH

Frozen cardiac tissue from each group was used to determine the activity of the aconitase [E.C.4.2.1.3] by monitoring the $NADP^+$ reduction (340 nm) by isocitrate dehydrogenase [EC 1.1.1.42] upon addition of (in mM) 1 sodium citrate, 0.6 $MnCl_2$, 0.2 $NADP^+$ and 1 U·mL^{-1} isocitrate dehydrogenase [EC 2.7.11.5] as previously reported (Silva-Platas *et al.*, 2012). Membrane lipid peroxidation was analysed by measuring the generation of thiobarbituric acid-reactive substances (TBARS) and reduced GSH in heart extracts was quantified utilizing the GSH-Glo GSH assay from Promega (Madison, WI, USA). $NADP^+$ and NADPH in heart tissue was extracted under acidic (0.4 M HCl) or basic (carbonate buffer, pH 11) conditions and extracts were neutralized to pH 7.5. The quantification was carried out with the GloTM assay (Promega). Concentration was obtained creating a standard curve for each component and expressed in nmol·mg^{-1} protein.

cAMP and PKA activity assay

Heart homogenates were obtained from atria or ventricles in lysis buffer [(in mM) 20 MOPS, 50 β-glycerolphosphate, 50 NaF, 1 sodium vanadate, 5 EGTA, 2 EDTA, 1 DTT, 1 benzamidine, 1 PMSF, 1% NP40, 10 mg·mL^{-1} leupeptin and aprotinin] using a Polytron at 10 000 r.p.m. After centrifugation at 11 000× *g*, the supernatant was collected. cAMP levels were determined using complete ELISA kit (ENZO Life Sciences, Farmingdale, NY, USA) following manufacturer's instruction. PK activity was determined using PKA activity kit (ENZO Life Sciences) using 200 and 400 ng per well of the phospho-specific substrate antibody and the anti-rabbit IgG HRP conjugate respectively.

Western blots of phospholamban (PLB)

Heart homogenates from atria or ventricles (15 μg) were resolved by SDS-PAGE as previously described (Benkusky *et al.*, 2007). Blocked membranes were incubated at 4°C for 10 h in PBS-T with antibodies to PLB-pThr^{17} (1:5000; Santa Cruz Biotechnology, Santa Cruz, CA, USA) or anti-PBL (1:1000; Abcam, Cambridge, UK). Membranes were washed three times in PBS-T for 10 min. After washing, membranes were incubated with the respective secondary antibody anti-IgG (Millipore, Billerica, MA, USA) conjugated to HRP in PBS-T for 2 h. After washing three times for 10 min, protein–antibody reactions were detected using the Clarity Western ECL substrate (Bio-Rad, Hercules, CA, USA) and the UVP Image Acquisition System. The level of phosphorylation was expressed as the ratio of the intensities of the phospho-signal for each antibody to the anti-PLB signal.

Data analysis

Pooled data are presented as mean ± SEM. Single or paired Student's *t*-test was used to determine the statistical significance of the data. ANOVA test was used for comparisons among treatments. Pearson product-moment correlation was used for correlation among variables. $P \leq 0.05$ was considered statistically significant.

Materials

Ru_{360} (μ-oxo)bis(trans-formatotetramine ruthenium) was synthesized following the procedure described by Ying *et al.* (1991). Ru_{360} concentration after chemical synthesis was calculated from the molar extinction coefficient of the complex at 360 nm (ξ = e 2.6 × 10^4 M^{-1}·cm^{-1}), as described by others (Matlib *et al.*, 1998; Zazueta *et al.*, 1999). All other materials were from Sigma, except for Fluo-3AM and Rhod-2 that were supplied by Invitrogen.

Results

Ru_{360} – a specific blocker of MCU – decreases cardiac contractility and MVO_2

Acute effects of Ru_{360} on MPi and MVO_2 were analysed in the rat isolated heart preparation. Figure 1A shows a time course of Ru_{360} effect on heart contractility. MPi was measured in hearts of untreated controls (open circles) and in the presence of 5 μM Ru_{360} (solid circles). In the presence of Ru_{360}, cardiac contractility was rather slow and gradual; the diminution of MPi began within 10 min of perfusion, peaked between 30 and 45 min and was still significant at 60 min. The time for half-inhibition ($t_{0.5}$) by Ru_{360} is given in Table 1. Panel B of Figure 1 illustrates the representative recordings of heart performance in control (left) and 5 μM Ru_{360} (right) perfused hearts at 30 min. Ru_{360} treatment produced a significant reduction in heart contractility, shown as a decrease (45%) of left ventricular pressure (LVP), an increase in HR of 20%, and a decrease in 30% MPi and 18% MVO_2, compared with the control. Increasing doses of Ru_{360} were administered via the perfusate solution of isolated heart preparations during 30 min. Figure 2A shows the dose-dependent effects of Ru_{360} on MPi and MVO_2. The maximal inhibitory effect of Ru_{360} was observed at 200 μM and the IC_{50} is shown in Table 1. Panel B shows that, in Ru_{360}-treated hearts, relaxation rate decreased whereas the contraction rate was preserved. In addition, the kinetics parameters of Ru_{360} showed an 11-fold diminution on IC_{50} on relaxation versus contraction rate (Table 1), suggesting a preferential effect of Ru_{360} on cardiac relaxation. Figure 2C shows a concentration-dependent effect of Ru_{360} on Ca^{2+} transients of isolated cardiomyocytes. Ventricular myocytes perfused with Tyrode buffer and stimulated at 1 Hz exhibit normal contraction and peak Ca^{2+} transients before treatment with 0.5 μM Ru_{360} (upper panel). The maximal inhibitory effect of Ru_{360} was observed at 50 μM and the half-maximal inhibitory concentration (IC_{50}) was 7.1 ± 0.9 μM. Perfusion of the cells with 15 μM Ru_{360} for up to 30 min significantly decreased the amplitude of $[Ca^{2+}]_c$ and cell shortening (not shown). The results suggest that Ru_{360} at submicromolar concentration does not affect normal $[Ca^{2+}]_c$ transients and shortening of isolated cardiac myocytes. Panel D shows HR response. As illustrated, Ru_{360} caused a dose-dependent increase in the HR. This was evident as early as 10 min following administration of Ru_{360}. This interesting finding might indicate that changes in mitochondrial Ca^{2+} transport will affect the cardiac pacemaker automaticity in accordance to a recent paper (Yaniv *et al.*, 2012). We characterized the effects of Ru_{360} on PKA and Ca^{2+}/calmodulin-dependent PK (CaMKII) signalling as this signalling pathway regulates the firing rate of the sinoatrial node action potential (Lakatta *et al.*, 2010). First, we measured cAMP levels and PKA activity in atrial tissue treated with isoprenaline (100 nM) during 10 min and observed a significant twofold increase in cAMP (Supporting Information Fig. S1). Ru_{360} treatment did not affect the cAMP production and PKA activity following isoprenaline stimulation. Perfusion with isoprenaline also increased CaMKII activity, shown as phosphorylated PLB-Thr^{17} (Supporting Information Fig. S1C). Ru_{360} treatment increased phosphorylated PBL in response to isoprenaline, indicating that the CaMKII pathway increased in Ru_{360}-treated atrial tissue, causing a positive chronotropic effect.

Spermine (Spm), an allosteric activator of mitochondrial Ca^{2+} uptake, causes a positive inotropic effect in rat heart

To support the identity of MCU as the molecular entity responsible for the effects described above, we performed additional experiments with a known MCU agonist. Rat isolated hearts were perfused with various concentrations of Spm, a permeable activator of MCU (Brunton *et al.*, 1990; Gunter and Pfeiffer, 1990). As shown in Figure 3A, Spm

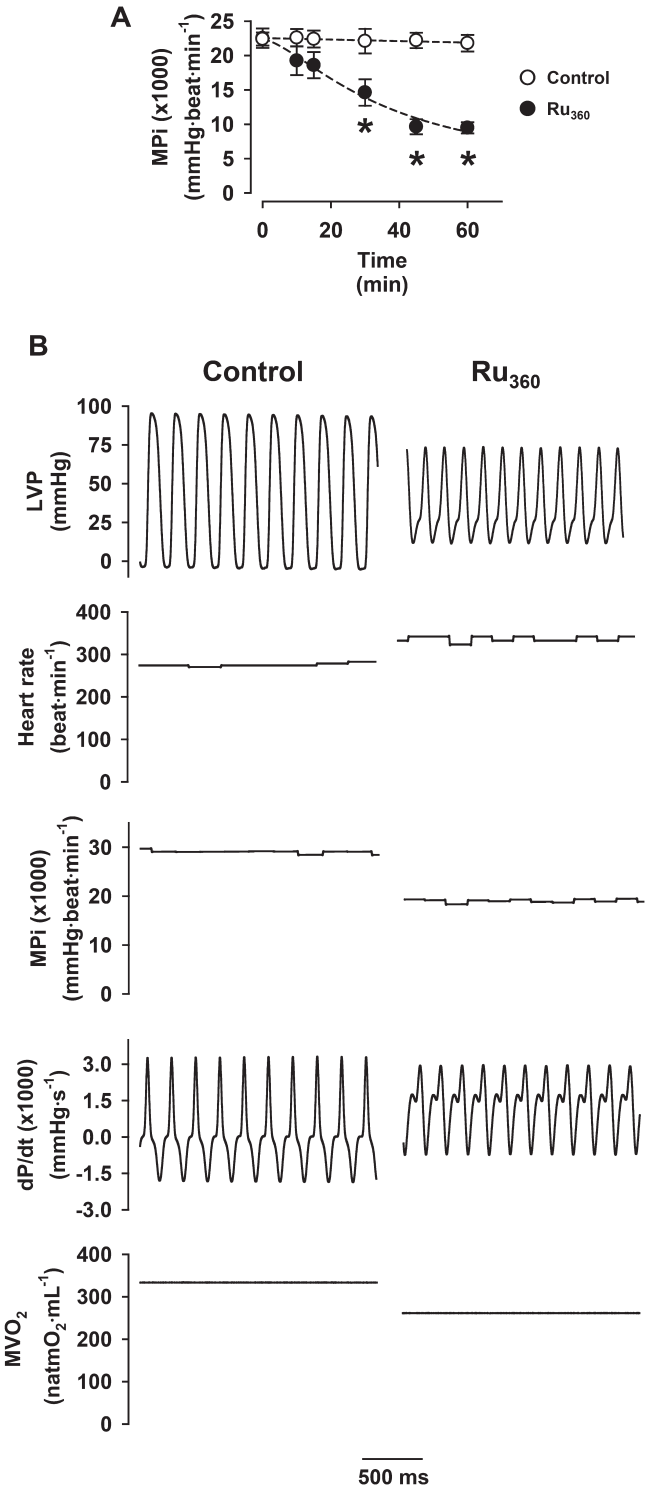

Figure 1

Ru_{360} has negative inotropic effects on unstimulated isolated rat hearts. Panel A shows a time course of Ru_{360} effect on heart contractility. MPi was measured in untreated hearts (controls) or withRu_{360} (5 μM). In the presence of Ru_{360}, cardiac contractility diminished gradually after 10 min of perfusion and reached the lowest at 45 min. The time for half-inhibition ($t_{0.5}$) of Ru_{360} was 21 ± 3 min. Panel B shows representative recordings of heart performance at 30 min of perfusion in control (left) and 5 μM Ru_{360} (right) hearts. Ru_{360} treatment produced a significant reduction in heart contractility, indicated by the decrease of LVP accompanied by a slight increase in heart rate. The MPi and MVO_2 were lower after RU_{360} than in controls. Values represent mean ± SEM ($n = 7$). *$P \leq 0.05$, significantly different from control.

(50 μM) increased the MPi in a time-dependent manner, ($t_{0.5}$ inTable 1), whereas the untreated controls showed no change. The maximal stimulation was achieved and sustained after 5–10 min of Spm perfusion. Therefore, at 10 min of Spm treatment, we obtained a dose-dependent positive inotropic effect on MPi and MVO_2, with half-maximal effective concentration (EC_{50}) around 55 ± 7 and 136 ± 48 μM respectively (Figure 3B). The kinetic properties of Spm on relaxation and contraction rate had shown a similar EC_{50} (Table 1) suggesting positive inotropic and lusitropic effects. Activation of Ca^{2+} uptake from mitochondria by Spm progressively reduced the HR to 16% control over a 10 min period at 2 mM. Note that the effects of Spm on chronotropy were the opposite od those after the MCU inhibitor (Figure 3C). In Figure 4A, upper panel, we present a time course of MPi in control hearts. In the presence of Spm (50 μM), a rapid increase in MPi was observed (Figure 4A, middle panel). Pretreatment for 30 min with 5 μM Ru_{360} in the perfusate blocked the Spm-positive inotropic effect (Figure 4A, lower panel). Spm treatment increased MPi and MVO_2 by 35 and 40% respectively but Ru_{360} still decreased the stimulation by Spm (Figure 4B and C). In addition, perfusion with Spm (50 μM) increased both PDHa activity and $[Ca^{2+}]_m$ and these changes were almost totally prevented by Ru_{360} treatment (Figure 4D and E). Simultaneous co-treatment of Spm and Ru_{360} failed to block Spm-positive inotropic effect (data not shown) probably due to slow and gradual Ru_{360} effect. All together, these results suggest that the positive inotropic effect of Spm could be dependent on mitochondrial calcium transport.

Ru_{360} decreased the inotropic effect of isoprenaline in isolated hearts

The role of MCU in cardiac contractility was further characterized by applying isoprenaline to isolated hearts to activate β_1-adrenoceptors, with or without Ru_{360}. As shown in Figure 5A, isoprenaline increased contractility concentration-dependently, but Ru_{360}-treated hearts failed to increase MPi, HR, +dP/dt and –dP/dt in response to isoprenaline (Figure 5B and C). In ventricular tissue, we examined whether Ru_{360} action was mediated by activation of PKA signalling. Although isoprenaline (100 nM) increased cAMP (Figure 6A). Ru_{360} treatment did affect this response. Similarly, the PKA and CaMKII activity after isoprenaline was not affected by Ru_{360} (Figure 6B and C).

Ru_{360} decreased MVO_2 and $[Ca^{2+}]_m$ during responses to β-adrenoceptor stimulation

During isoprenaline treatment, the amplitude of cytosolic Ca^{2+} transient increases, and with it the energy demand in the cell. To exclude the possibility that Ru_{360} may have negatively affected cytosolic Ca^{2+} handling in ventricular cells, and

Table 1

Dose and time dependent constants on hearts treated with mitochondrial Ca^{2+} uptake modulators

		Time-dependent constants (min)	
		Ru_{360}	Spm
MPi (×1000) (mmHg·beat·min^{-1})	$t_{0.5}$	21 ± 3	1.7 ± 0.3
		Dose-dependent constants (μM)	
MPi (×1000) (mmHg·beat·min^{-1})	IC_{50}	7 ± 3	–
	EC_{50}	–	55 ± 7
MVO_2 (μmolO_2·min^{-1}·g^{-1})	IC_{50}	17 ± 9	–
	EC_{50}	–	136 ± 48
+dP/dt (×1000)	IC_{50}	15 ± 3	–
	EC_{50}	–	48 ± 9
–dP/dt (×1000)	IC_{50}	1.3 ± 0.5	–
	EC_{50}	–	21 ± 6
Peak Ca^{+2} transient ($\Delta F/F_0$)	IC_{50}	7.1 ± 0.9	–

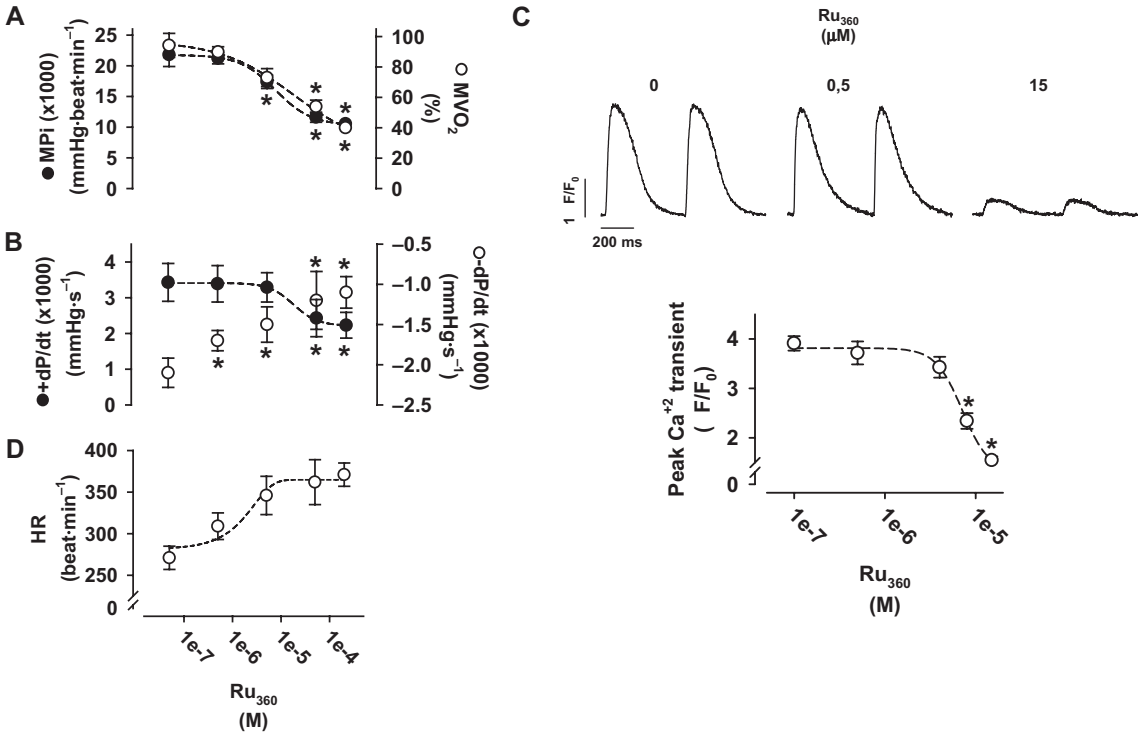

Figure 2

The effects of Ru_{360} on heart contractility, oxygen consumption, chronotropy and Ca^{+2} transient are concentration-dependent. Increasing doses of Ru_{360} were administered via the perfusate of isolated heart preparations during 30 min. Panel A shows the concentration-dependent effect of Ru_{360} on MPi and MVO_2. The maximal inhibitory effect of Ru_{360} was observed at 200 μM and the IC_{50} for Ru_{360} was 7 ± 3 μM. Panel B shows the +dP/dt and –dP/dt in Ru_{360}-treated hearts. The relaxation rate decreased with 5 μM Ru_{360}, while preserving the contraction rate (3.4 ± 0.5 vs. 3.3 ± 0.4 (×1000) mmHg × s^{-1}). Panel C shows the effect on Ca^{+2} transients in isolated cardiomyocytes. Upper panel represents a representative recording of Ca^{+2} transients at 0 (vehicle), 0.5 and 15 μM of Ru_{360}. Lower panel shows the concentration-dependent effect on the peak Ca^{+2} transient before 30 min of treatment with Ru_{360}. The half inhibitory dose is 7.1 ± 0.9 μM. In panel D, treatment with Ru_{360} caused a concentration-dependent increase in the HR, evident as early as 10 min after starting perfusion with Ru_{360}. Values are the mean ± SEM (at least n = 5 experiments for each dose). *$P \leq 0.05$, significantly different from baseline.

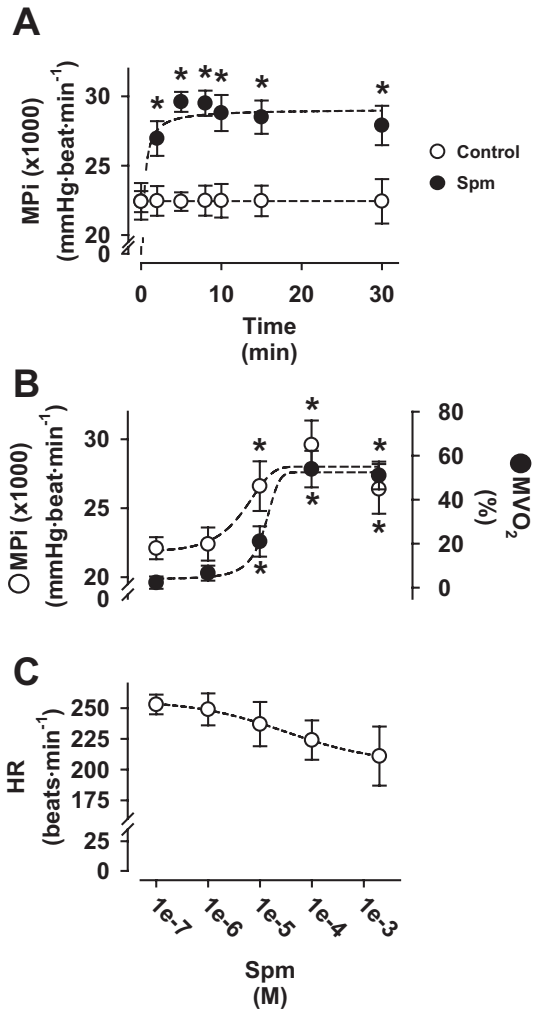

Figure 3

Spermine (Spm), an allosteric activator of mitochondrial Ca^{2+} uptake, exerted positive inotropic effects on rat heart. Isolated hearts were perfused with various concentrations of Spm a permeable activator of the MCU. In panel A, Spm (50 μM) increases the MPi in a time-dependent manner, with a time for half-effective ($t_{0.5}$) of 1.7 ± 0.3 min. Untreated controls did not change. The maximal stimulation was achieved and sustained after 5–10 min of Spm perfusion. In panel B, the concentration-dependent, positive inotropic effect of Spm, measured at 10min, on MPi and MVO_2, with EC_{50} around 55 ± 7 and 136 ± 48 μM respectively. Heart rate did not change importantly during Spm perfusion (panel C). Values are the mean ± SEM (n = 5–6 experiments for each treatment). *$P \leq 0.05$, significantly different from control.

consequently reduced MPI and MVO_2, we recorded Ca^{2+} transients in isolated hearts from mice. Isolated hearts were loaded with Rhod-2 and electrically evoked Ca^{2+} transients in epicardial ventricular myocytes were visualized with PLFF microscopy. Figure 6, panel D, shows representative recordings of control and Ru_{360}-treated hearts. The Ca^{2+} transients recorded in control hearts exhibited normal contraction and peak Ca^{2+} transients before treatment with 0.5 μM Ru_{360}. Averaged data (Figure 6, panel D) indicate a similar effect on Ca^{2+} transient amplitude in control and Ru_{360}-treated hearts during extracellular Ca^{2+} increase. The duration of Ca^{2+} transient at half-maximum amplitude (t_{50}) was not different between groups (data not shown). Thus, Ru_{360} treatment did not reduce contractile properties through negative effects on Ca^{2+} handling. During the perfusion with isoprenaline, MVO_2 increased 2.7-fold but isoprenaline in Ru_{360}-treated hearts (0.5 μM) failed to increase MVO_2 (Figure 7A). In panel B, we show a linear relationship between MPi and MVO_2 that represents cardiac efficiency, in the two sets of heart [slope in control hearts = 0.53 ± 0.02 vs. Ru_{360}-treated slope (r) = 0.98 ± 0.08, $P < 0.01$].

Panels C, D show the PDH activity (PDHa) in heart homogenates and $[Ca^{2+}]_m$ in isolated mitochondria respectively. During β-adrenoceptor stimulation, PDHa activity increased fivefold versus control. Remarkably, PDHa activity in Ru_{360}-treated hearts with isoprenaline was 43% lower than in control hearts treated with isoprenaline. $[Ca^{2+}]_m$ was significantly increased by isoprenaline (2.5-fold) compared with control hearts. This effect was almost blocked in the Ru_{360}-treated hearts. There were no significant changes in myocardial PCr and ATP after isoprenaline in control or Ru_{360}-treated hearts (panels E, F). These findings suggest that the feedback mechanism between ATP demand (e.g. ATPase activity in the myofibrils) and production in the mitochondria is highly buffered (Katz *et al.*, 1989). Even the slight changes in the Ru_{360} + isoprenaline hearts may suggest a local diminution that affects heart contractility.As shown in Figure 8, we found an exponential relationship between MPi and PDHa activity or MVO_2 suggesting that MPi was dependent on MCU activity. Changes in PDHa activity have shown that modification on MCU activity caused variations in cardiac contractility (r = 0.961, P = 0.002). Modifications of MVO_2 had shown a similar relationship with MCU agonist or blockers (r = 0.962, P = 0.002). All these data suggest that $[Ca^{2+}]_m$ must play a role in the feedback mechanism between energy production and MPi in the heart, and that the MCU plays a relevant role on this metabolic–mechanical coupling, in particular during mechanical overload.

The negative inotropic effect induced by Ru_{360} is not dependent on oxidative stress

A recent paper identified a previously unrecognized role of mitochondrial Ca^{2+} uptake for the control of mitochondrial reactive oxygen species (ROS), triggered by oxidation of NADPH (Kohlhaas *et al.*, 2010). This ROS formation was potentiated when mitochondrial Ca^{2+} uptake was blocked with Ru_{360}. To explore this as a possible mechanism for impaired response to β-adrenoceptor stimulation in Ru_{360}-treated hearts, we measured $NADP^+$/NADPH, GSH levels and TBARS formation. We observed that neither Ru_{360}, Spm nor isoprenaline treatment elicited significant pro-oxidant action on isolated hearts; and differently from Kohlhaas *et al.'s* (2010) results on isolated cells, we found that in Ru_{360}-treated hearts the $NADP^+$/NADPH ratio did not change (control 1.1 ± 0.1; Ru_{360} treatment (0.5 μM) 0.9 ± 0.07; ISO (1 nM) 1.2 ± 0.02; Ru_{360} treatment +ISO 1.3 ± 0.02 nmol·mg^{-1}), and neither did GSH levels (Ru_{360} treatment 1.7 ± 0.6; Spm (50 μM) 1.5 ± 0.8; ISO 2.2 ± 0.5 nmol·mg^{-1}). The sensitivity of aconitase activity was not diminished under these conditions (Ru_{360} treatment 47 ± 5; Spm 58 ± 4; ISO 42 ± 4 nmol NADPH per min·mg^{-1}) and there was no evidence for oxidative damage to

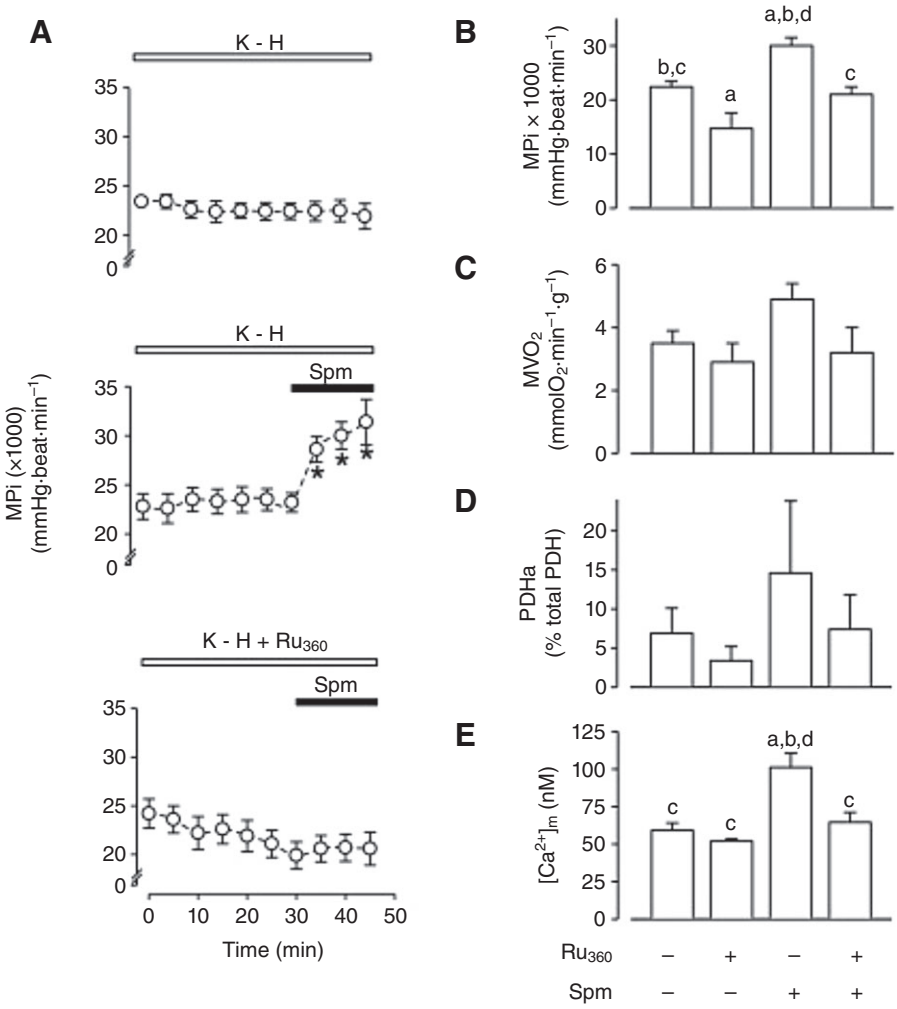

Figure 4

The stimulatory effect of spermine (Spm) in heart contractility is prevented by the early perfusion of Ru_{360}. Control values of MPi are represented in panel A, upper figure. In the presence of Spm (50 μM), MPi rapidly increased (Figure A, middle panel). Pretreatment with Ru_{360} (5 μM) in the perfusate blocked the positive inotropic effects of Spm (Figure A, lower panel). Comparisons made for MPi and MVO_2 of data extracted from panel A experiments are represented in panels B and C respectively. Significant differences are presented as (a) versus control, (b) versus 5 μM Ru_{360} treatment, (c) versus Spm treatment, and (d) versus Ru_{360} + Spm treatment. Direct measurements of pyruvate dehydrogenase activity (PDHa) in heart homogenates at the end of perfusion protocol are presented in panel D. Intramitochondrial calcium was determined in mitochondria isolated from hearts at the end of perfusion protocol (panel E). Values are the mean ± SEM (n = 5–6 experiments for each treatment). *$P \leq 0.05$, significantly different from control, ANOVA.

phospholipids of the membranes, as assayed by TBARS (Ru_{360} treatment 3.3 ± 0.9; Spm 2.5 ± 0.3; isoprenaline 2.8 ± 0.4 nmol TBARS per mg). According to these data, there was a decrease of $[Ca^{2+}]_m$ but this was not accompanied by an increased ROS production.

Discussion and conclusions

In this study, we provided evidence that supported the role of the MCU as a key regulator in cardiac contractility as well as defining its critical role in β-adrenoceptor stimulation. First, we found that, in an isolated heart model, Ru_{360}, a selective inhibitor of MCU, induced progressive and sustained negative inotropic effects. Second, in the same model, Spm, an MCU agonist, exerted positive inotropic effects that were blocked by Ru_{360}. Finally, the inotropic effects induced by β-adrenoceptor stimulation were partly blocked by the addition of Ru_{360}. This effect in ventricular tissue was not mediated by changes in PKA or CaMKII signalling. Taken together, these findings showed that MCU inhibition lowered responses to β-adrenoceptor stimulation, resulting from uncoupling of workload and production of energetic phosphate metabolites. Our results support the hypothesis that coupling between workload and energy supply is partly dependent on MCU activity.

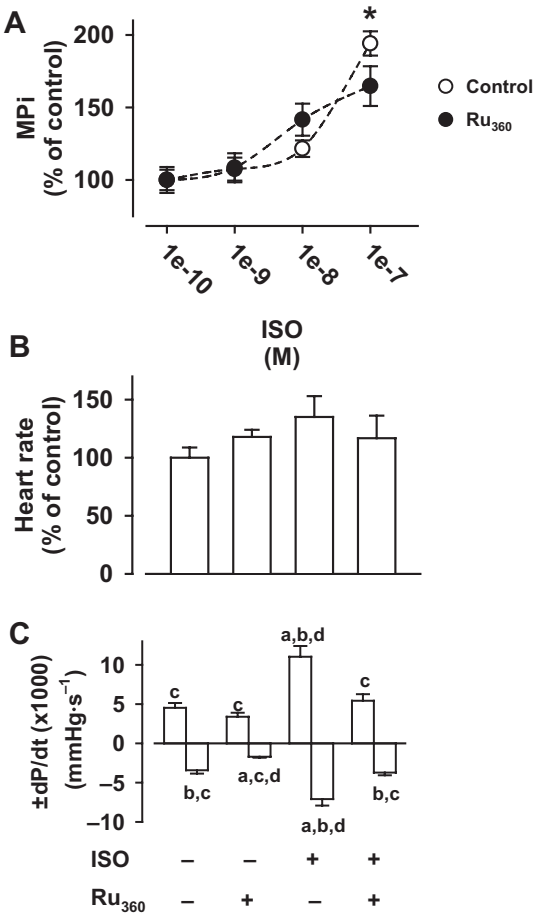

Figure 5

Ru_{360} decreases the inotropic effect of isoprenaline in isolated hearts. Isolated hearts were treated with various concentrations of isoprenaline (ISO), with or without Ru_{360} (panel A); data are shown at 30 min of perfusion.Treatment with isoprenaline increased the contractility in a concentration-dependent manner. Early perfusion with 0.5 μM Ru_{360} blocked the full inotropic response to isoprenaline. Panels B and C show HR and relaxation and contraction rate (±dP/dt) of isolated perfused hearts treated with isoprenaline (100 nM) with or without Ru_{360}. The increased MPi, chronotropy and lusitropy (–dP/dt) triggered by isoprenaline were lower in Ru_{360}-treated hearts. Values are the mean ± SEM (n = 5–6 experiments for each treatment). Significant differences ($P \leq 0.05$) are presented as (a) versus control, (b) versus Ru_{360} treatment, (c) versus isoprenaline treatment, and (d) versus Ru_{360} + isoprenaline treatment; ANOVA.

The role of MCU in cardiac contractility

Ru_{360} is commonly used as a specific inhibitor of the MCU with the purpose of studying mitochondrial Ca^{2+} transport and its physiological role. For example, when Ru_{360} (5–10 μM) is added to the external solution, it inhibits mitochondrial Ca^{2+} uptake in intact rat (Belmonte and Morad, 2008) and ferret myocytes (Zhou and Bers, 2002; Jo *et al.*, 2006), without affecting sarcoplasmic reticulum Ca^{2+} transport, L-type Ca^{2+} channels or sarcolemmal Na^+/Ca^{2+} exchanger activity (Matlib *et al.*, 1998). Others have found that Ru_{360} does not appear to enter into adult (Maack *et al.*, 2006) or neonatal (Bell *et al.*, 2006) cardiomyocytes because it had no effect on the mitochondrial Ca^{2+} transients observed in these cells.

However, Matlib *et al.* (1998) measured the uptake of radioactive $^{103}Ru_{360}$ into isolated rat ventricular myocytes and found a slow uptake. Over 30 min, the authors estimated the cytosolic [Ru_{360}] to be 100 nM, which would be sufficient to completely inhibit MCU. Experiments on ferret myocytes under similar conditions showed that incubation for 30 min with 10 μM Ru_{360} inhibited Ca^{2+} uptake into mitochondria induced by cell depolarization (Zhou and Bers, 2002). In isolated guinea pig ventricular myocytes, 10 μM Ru_{360} largely attenuated both the metabolic response and mitochondrial Ca^{2+} transients (Jo *et al.*, 2006).

In this regard, our experiments on Ru_{360}-treated isolated hearts also showed a slow effect with a time constant (21 ± 3 min), similar to previous experiments in intact cardiomyocytes (Figure 1 and Table 1). Importantly, several observations suggest that the use of Ru_{360} is associated with cardiac protection in conditions where cell injury is produced by Ca^{2+} overload. For example, the addition of Ru_{360} protects hearts or myocytes from Ca^{2+} overload at concentrations ranging from 0.2 to 6 μM (García-Rivas *et al.*, 2005; Zhang *et al.*, 2006; Correa *et al.*, 2007; Ragone and Consolini, 2009). Pretreatment of rat isolated hearts with Ru_{360} provided protection against reperfusion injury, as shown by mechanical parameters, infarct size and intracellular enzymes release (García-Rivas *et al.*, 2005, 2006; Shintani-Ishida *et al.*, 2012). Further, we previously reported that lower concentrations of Ru_{360} were required to reduce mitochondrial matrix Ca^{2+}, indicating that Ru_{360} partly blocks MCU *ex vivo* (García-Rivas *et al.*, 2005). In the present study, we observed that Ru_{360} produced a potent and gradual negative effect on cardiac workload and MVO_2 (IC_{50} = 7 ± 3 μM). Additionally, activation of the MCU with Spm increased the cardiac workload and pretreatment with Ru_{360} abolished this effect of Spm, suggesting that mitochondrial Ca^{2+} uptake has a role on modulating cardiac workload (Figure 3C). Recently, the molecular nature of the channel has been identified as a result of progress in genome sequencing. An RNAi screening allowed the identification of the MCU protein, and other MCU regulator proteins known as MICU1 and MICU2, MCUR1, MCUb and EMRE (Perocchi *et al.*, 2010; Baughman *et al.*, 2011; De Stefani *et al.*, 2011; Mallilankaraman *et al.*, 2012; Raffaello *et al.*, 2013; Sancak *et al.*, 2013). In this regard, at the cellular level, overexpression of MCU increased the rate of Ca^{2+} uptake and this sensitized the cells to death following Ca^{2+} overload (Baughman *et al.*, 2011); these results were consistent with pharmacological studies using Ru_{360} (Correa *et al.*, 2007). But more importantly, recent observations from our laboratory indicated that MCU protein is expressed differentially in the normal human heart and in disease states (G. García-Rivas *et al.*, unpublished). A very recent study by Pozzan's group used genetic silencing of the MCU in neonatal cardiomyocytes, and observed that, during spontaneous pacing, $[Ca^{2+}]_m$ decreased while $[Ca^{2+}]_c$ and contraction increased. Therefore, in neonatal myocytes, these data support the idea that MCU could serve as a spatial Ca^{2+} buffer and thus affect the magnitude and the amplitude of the increase of systolic Ca^{2+} (Drago *et al.*, 2012). However, in the present study, blocking MCU with Ru_{360} significantly reduced contraction. Dissimilarities between the earlier study and our

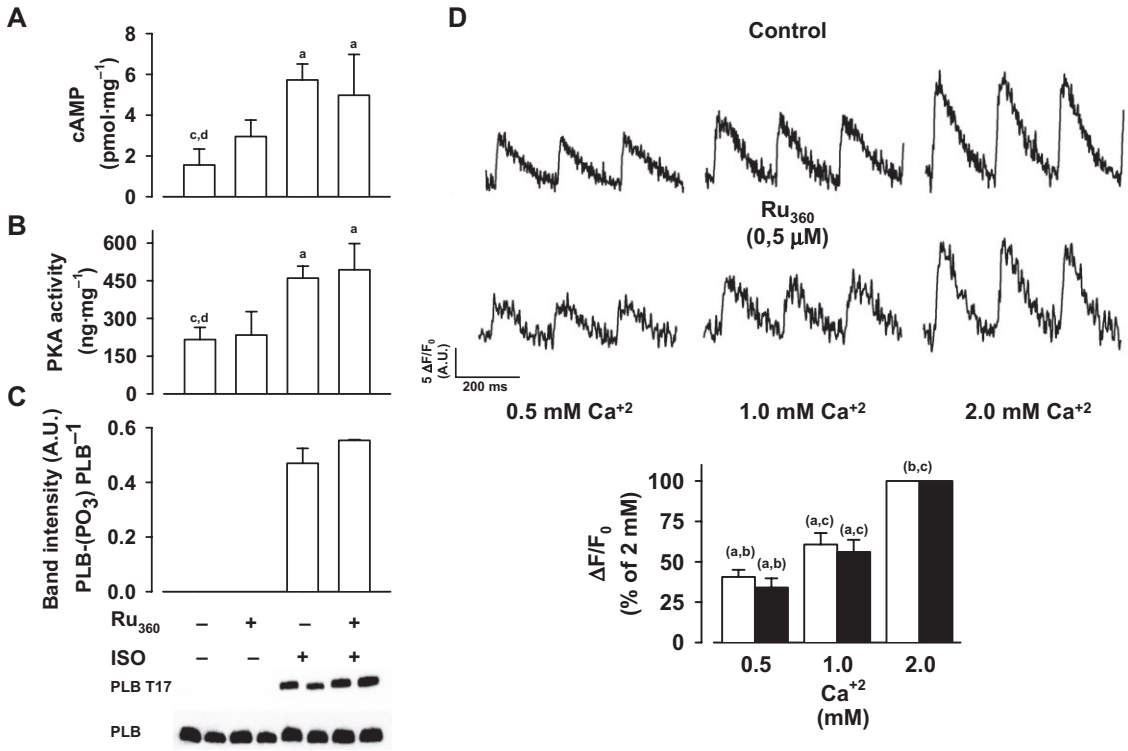

Figure 6

Integrity of downstream β-adrenoceptor signalling and intracellular Ca^{2+} handling during Ru_{360} perfusion. In panel A, the intracellular content of cAMP in homogenates of ventricles from hearts perfused with isoprenaline (ISO; 100 nM) for 10 min was increased fourfold. Ru_{360} treatment (0.5 μM) for 30 min did not affect cAMP production in response to isoprenaline stimulation. In panel B, PKA activity in hearts perfused with isoprenaline was not affected by Ru_{360}. In panel C, Western blots of the phosphorylation of phospholamban at Thr^{17} are shown. In panel D, isolated mouse hearts loaded with Rhod-2 were used to evaluate intracellular calcium in the epicardial layer, using PLFF microscopy. Upper recording shows the trace of the transient for control and lower recording (0.5 μM) Ru_{360} perfusion. Ca^{2+} is increased during perfusion to verify the experiment outcome. Inset panel shows the transient amplitude normalized to the value of 2 mM Ca^{+2} for the transient for control and for Ru_{360} treated hearts. Values are the mean ± SEM (n = 4–7 experiments for each treatment). Significant differences ($P \leq 0.05$) are presented as (a) versus control, (b) versus Ru_{360} treatment, (c) versus isoprenaline treatment, and (d) versus Ru_{360} + isoprenaline treatment.

study reflect not only differences between adult and neonatal cardiac cells, but also the different experimental models employed, that is, isolated single pacemaker cells in the earlier study and intact hearts in the present study. A very useful tool for obtaining direct insights into the role of MCU in cardiac contractility in the whole heart would be the specific knockout animal model for this protein, as has recently described (Pan *et al.*, 2013).

β-adrenoceptor stimulation and MCU activity

The heart needs a cellular mechanism to increase and or balance the PCr/ATP ratio to meet the demand for energetic metabolites, for instance during the increased workload produced by β-adrenoceptor stimulation. Early studies in isolated mitochondria found that the ADP/ATP ratio was the main regulator of ATP production, but studies in beating hearts found that the ratio between PCr/ATP did not change in *ex vivo* hearts, even during large increases in workload (Portman *et al.*, 1989).

The findings of the present study are in support of the latter idea that, independent of increased workload caused by β-adrenoceptor stimulation, PCr/ATP levels in beating hearts were remarkably constant (Figure 7E and F). In contrast, an exponential correlation between PDH activity and MCU activity was found (Figure 8), indicating that Ca^{2+} could activate mitochondrial dehydrogenases like PDH. Our findings support the hypothesis that an increase in the supply of reducing equivalents, in the form of NADH and $FADH_2$, would increase ATP production (Jo *et al.*, 2006), and is consistent with a model in which $[Ca^{2+}]_i$ regulates both the utilization of energetic metabolites by the work-producing ATPases, as well as the mitochondrial production of ATP.

In this study, we found that MCU inhibition restricted workload stimulation due to decreased Ca^{2+} uptake into mitochondria (Figure 7D); however, we observed that cardiac efficiency in Ru_{360}-treated hearts (Figure 7B) was energetically improved. This exciting result could imply that cardiac workload and PCr/ATP ratio were maintained even though no increase in $[Ca^{2+}]_m$ occurred, and suggested that increases in $[Ca^{2+}]_m$ play an alternative role under stimulation workload. In this regard, Territo *et al.* (2000) demonstrated that Ca^{2+} added to previously Ca^{2+}-depleted cardiac mitochondria rapidly increased the velocity of ATP production by the F_1-F_0-

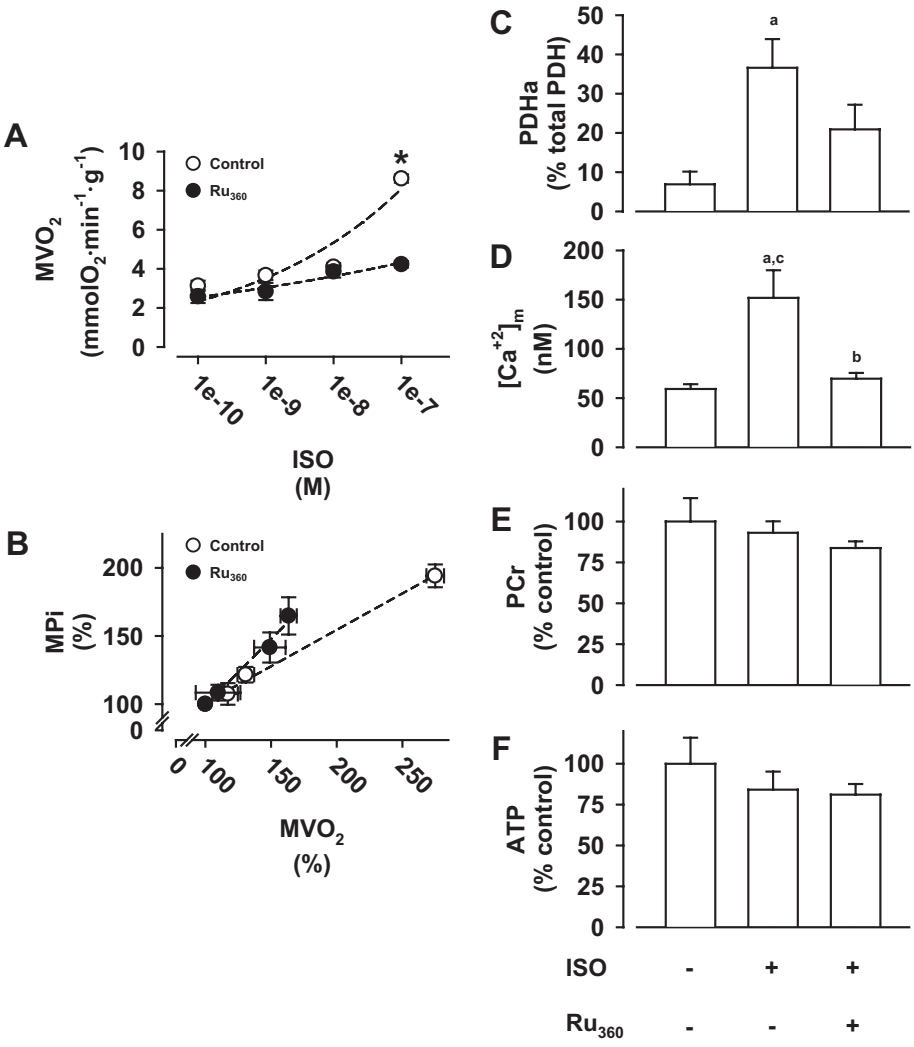

Figure 7

Ru_{360} decreases oxygen consumption and $[Ca^{2+}]_m$ during β-adrenoceptor stimulation. Isolated hearts were treated with increasing concentrations of isoprenaline (ISO) with or without Ru_{360} (0.5 μM). As shown in panel A, isoprenaline (ISO) increased MVO_2 and this response was absent in Ru_{360}-treated hearts. Panel B shows the relationship between MPi and MVO_2. Panels C and D show the pyruvate dehydrogenase activity (PDHa) in heart homogenates and $[Ca^{2+}]_m$ in isolated mitochondria respectively. PDHa activity increased after isoprenaline and this increase was blocked by Ru_{360}. $[Ca^{2+}]_m$ was also increased by isoprenaline and this effect was almost abolished by Ru_{360}. In panels E, F, isoprenaline did not change myocardial PCr or ATP and Ru_{360} did not affect this lack of response. Values are the mean ± SEM (n = 5–6 experiments for each treatment). Significant differences ($P \leq 0.05$) are presented as (a) versus control, (b) versus isoprenaline treatment, and (c) versus Ru_{360} + isoprenaline treatment; ANOVA.

ATPase modulating the ΔΨ (Territo *et al.*, 2000). Thus, Ca^{2+} is capable of increasing the capacity of ATP production by the F_1-F_0-ATPase at a constant driving force simultaneously with the increased delivery of NADH. Similar to our results, the half-maximal effect of Ca^{2+} was inhibited by MCU blockers, indicating matrix dependence of the Ca^{2+} effect (Territo *et al.*, 2000; Sun *et al.*, 2009). Furthermore, it has been shown that ΔΨ decreases during Ca^{2+} mobilization in HeLa cells (Poburko *et al.*, 2011). Ca^{2+} transport to mitochondria can elevate respiration possibly due to an increase in the mitochondrial matrix volume, which in turn can produce swelling in isolated mitochondria (Halestrap, 1987). However, in isolated cardiomyocytes, the increase in $[Ca^{2+}]_c$ during low electrical stimulation (1 Hz) did not increase mitochondrial volume, suggesting that, at resting or low workloads, mitochondrial swelling does not serve to facilitate this purpose (Yaniv *et al.*, 2011). Nevertheless, during increased workload after β-adrenoceptor stimulation, volume-activated Ca^{2+} transport into mitochondria might increase in response to increases in myofilament strain to couple ATP supply and demand. Therefore, it is possible that during cardiac workload, an increase in Ca^{2+} serves to facilitate this purpose. Possibly, Ru_{360}-treated hearts, which are resistant to mitochondrial swelling and permeability transition (García-Rivas *et al.*, 2006), could explain the improvement in efficiency of cardiac workload.

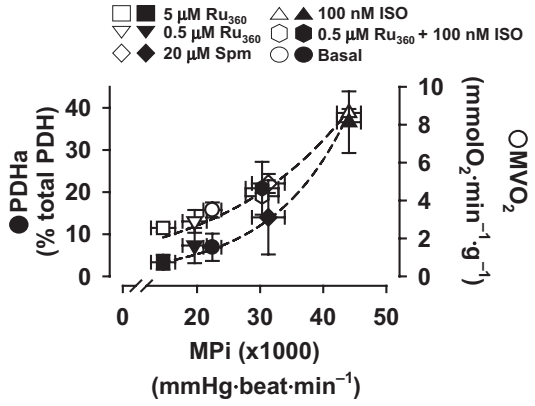

Figure 8

MCU activity couples mechanical to metabolic responses in the isolated heart. Changes in pyruvate dehydrogenase (PDHa) activity are associated with the modification of MCU activity and these with variations in cardiac contractility ($r = 0.961$, $P = 0.002$). Modifications of oxygen consumption (MVO_2) show a similar relationship with MCU agonist or blockers ($r = 0.962$, $P = 0.002$). The MCU activity was modified using 5 μM and 0.5 μM Ru_{360}, 20 μM spermine, 100 nM isoprenaline, 0.5 μM Ru_{360} + 100 nM isoprenaline. Pearson product-moment correlation was used to test for correlation among variables. Values are the mean ± SEM (n = 5 experiments for each treatment).

Recently, Lakatta's group suggested that mitochondrial Ca^{2+} transport modulated chronotropism in pacemaker cells (Yaniv *et al.*, 2012). These results indicated that mitochondrial Ca^{2+} dynamics acted as a buffer of cytosolic Ca^{2+}, which therefore affected sarcoplasmic reticulum Ca^{2+} handling, leading to changes in spontaneous action potential. In accordance with those results, a similar effect of Ru_{360} on HR was documented in our study (Figure 2, panel D) and stimulates mitochondrial Ca^{2+} uptake with Spm that mimicked the bradycardic effect of CGP37157 (blocker of mitochochondrial Na^+/Ca^{2+} exchanger) on sinoatrial node cells. Chronotropic effects during β-adrenoceptor stimulation involve PKA and CaMKII-dependent phosphorylation of multiple proteins on sinoatrial node cells; furthermore, ATP production must increase to maintain high spontaneous action potential firing rate (Yaniv *et al.*, 2011). In this regard, a recent study from Yaniv *et al.* demonstrated that increased chronotropism was accompanied by an increase in MVO_2, ATP synthesis, $[Ca^{2+}]_m$ and cAMP. Similar to our results, when MCU was blocked by Ru_{360}, the increased chronotropism in response to isoprenaline was reduced.

Moreover, in atrial tissue treated with isoprenaline and Ru_{360}, CaMKII activity was increased (Supporting Information Fig. S1). However, in ventricular tissue, MCU inhibition did not modify PKA and CaMKII signalling (Figure 6). This differential tissue-specific result might have several explanations, including differential PKA/CaMKII-Ca^{2+} signalling between pacemakers and ventricular cardiomyocytes (Lakatta *et al.*, 2010). For instance, Joiner *et al.*, (2012) have recently demonstrated that MCU is a phosphorylation substrate CaMKII and that CaMKII phosphorylation increases MCU activity. Another possibility could be including differential expression levels of MCU and regulatory accessory proteins or NCXm between sinoatrial cells and ventricular cardiomyocytes.

The present findings demonstrate, for the first time, that the modulation of MCU in isolated hearts correlated with impaired metabolic responses to cardiac stimulation. The ability of the MCU inhibitor to improve energy efficiency may have several underlying mechanisms. (1) When an abrupt change of workload was simulated by β-adrenoceptor stimulation, ATP hydrolysis is increased, which increases the availability of ADP and P_i to stimulate ATP production. (2) Consumption of $\Delta\Psi$ by F_1-F_0-ATPase to stimulate electron transport, proton pumping, and the rate of NADH/$FADH_2$ oxidation at the onset of workload. (3) At the same time, the increase of amplitude of $[Ca^{2+}]_c$ transients promotes mitochondrial Ca^{2+} uptake through MCU, activating key dehydrogenases of the TCA cycle to supply reducing equivalents. Figure 9 is a schematic representation of the general idea on how $[Ca^{2+}]_c$ links sarcoplasmic reticulum and mitochondria during β-adrenoceptor stimulation , emphasizing the role of MCU.

Implications

Impairment of intracellular Ca^{2+} homeostasis and mitochondrial function has been implicated in the development of heart failure, and abundant studies have identified decreased cardiac energy levels and lower flux as consistent features of heart failure (Neubauer, 2007). Mitochondria isolated from failing hearts showed a reduced Ca^{2+} uptake and this was associated with a lower membrane potential and reduced activities of respiratory complexes (Lin *et al.*, 2007). Furthermore, recent work from O'Rourke's group demonstrated that inhibiting the mitochondrial Na^+/Ca^{2+} exchanger in a guinea pig model of heart failure increased $[Ca^{2+}]_m$ and activation of Ca^{2+}-dependent dehydrogenases, such as PDH. It is likely to restore ATP levels in the failing hearts regulating $[Ca^{2+}]_m$ (Sullivan *et al.*, 2006; Liu and O'Rourke, 2008). In addition, Michels *et al.* (2009) showed in the mitochondrial inner membrane from failing hearts that mitochondrial Ca^{2+} transport decreased in failing, compared with non-failing, human hearts. These results suggest that mitochondria from failing hearts were less effective in Ca^{2+} uptake and, consequently, in activation of Ca^{2+}-induced metabolism, which may explain, at least partly, the reduced myocardial energetic phosphate metabolite levels in heart failure. In this context, the MCU is a feasible target for treatment of conditions where ATP synthesis is impaired, such as in cardiomyopathies and heart failure. Activators of MCU could be used to increase $[Ca^{2+}]_m$ as this may be of benefit in heart failure., We therefore need pharmacological activators of MCU with greater specificity, given that Spm has other effects, for instance, on the regulation of cell proliferation and differentiation (Lee and MacLean, 2011).

On the other hand, the principal clinical manifestations of advanced heart failure are reduced systolic and diastolic functions, exacerbated by an excessive sympathetic activation and extensive abnormalities in β-adrenoceptor signalling (Braunwald and Bristow, 2000). In this regard, the reduced workload stimulation in MCU-blocked hearts suggests a condition similar to that observed in heart failure and indicates that MCU activity could lead to the uncoupling of mitochondrial metabolism from energy demand during cardiac stimulation. The recent identification

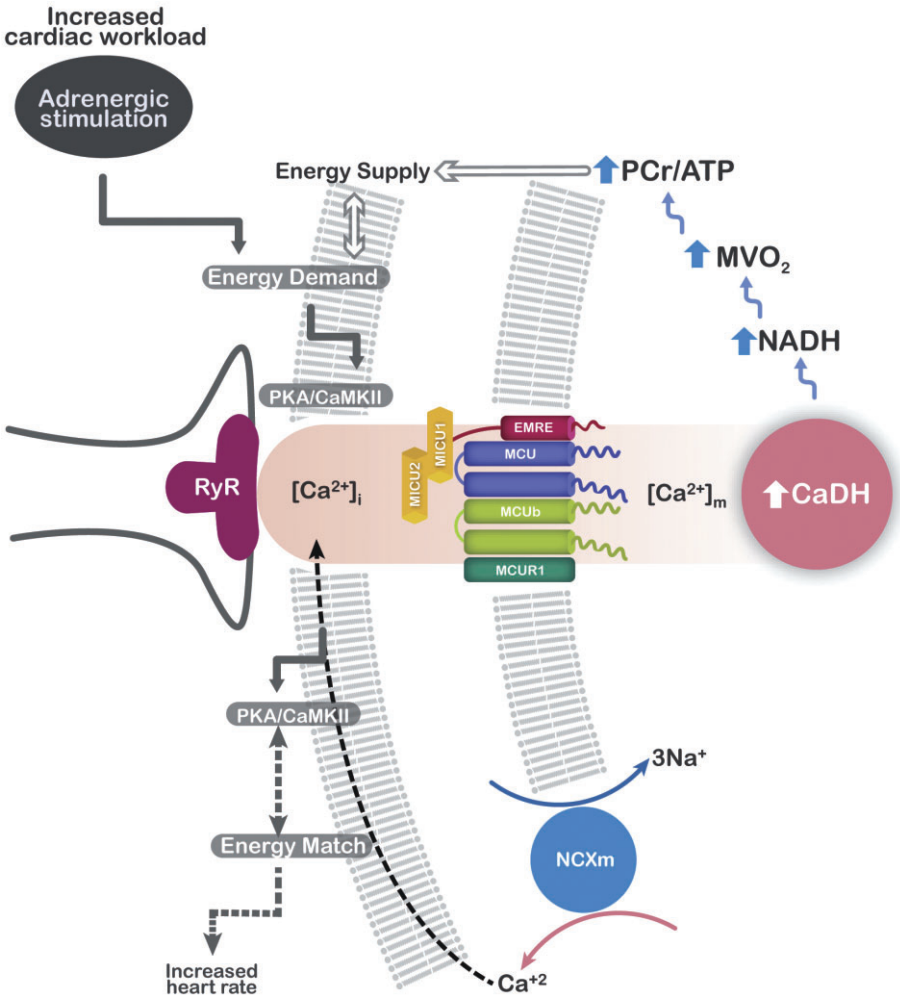

Figure 9

Scheme of the mechanism by which mitochondrial Ca^{2+} uniporter (MCU) contributes to cardiac workload. In ventricular myocytes, on β-adrenoceptor stimulation, cAMP-dependent PKA and Ca^{2+}/calmodulin-dependent PK (CaMKII) signalling is activated, which augments contractility and Ca^{2+} transients. In close proximity with mitochondria, ryanodine receptors (RyR) in the sarcoplasmic reticulum release Ca^{2+} into the mitochondrial intermembranal space and makes it available for uptake into the matrix by the MCU. This transmembrane protein consists of two transmembrane domains and a pore-forming region that contains Ser^{259}, a target for the inhibitory effect of Ru_{360} (Baughman *et al.*, 2011). In addition, mitochondrial Ca^{2+} uptake 1 and 2 (MICU1 and MICU2, respectively), MCUR1, MCUb and essential MCU regulator (EMRE) proteins act as regulators of this channel (Perocchi *et al.*, 2010; Mallilankaraman *et al.*, 2012; Raffaello *et al.*, 2013; Sancak *et al.*, 2013). The rise in intramitochondrial Ca^{2+} activates the Krebs cycle dehydrogenases (CaDH) increasing the capacity for the production of NADH. The respiratory chain oxidizes NADH and consumes O_2 (MVO_2) in order to establish the proton gradient for the production of ATP by oxidative phosphorylation. ATP is removed from mitochondria through the creatine kinase system. These events match the energy demand during the response to β-adrenoceptor stimulation . Therefore, inhibition of MCU impaired the cardiac workload. On the other hand, in sinoatrial node cells (dotted lines), mitochondrial Ca^{2+} flux [MCU and Na^+/Ca^{2+} exchanger (NCXm)] translates into a change in the action potential firing rate by effecting changes in cAMP/PKA/CamKII signalling, cytosolic Ca^{2+} and sarcoplasmic reticulum Ca^{2+} loading, which affects heart chronotropism.

of the molecular components of the MCU opens new possibilities in the clarification of the role of mitochondrial Ca^{2+} homeostasis on excitation–contraction and energetic coupling in normal and failing hearts and represents a fertile area of research in the future.

Acknowledgements

We acknowledge Dr Julio Altamirano for his insightful discussions concerning the manuscript, and Valeria Oropeza for the Figure 9 designs. This work was partially supported by Endowed Chair in Cardiology-Tec de Monterrey grant 0020CAT131 as well as Consejo Nacional de Ciencia y Tecnología-México grants 133591 and 131565 (G. G-R.). E. F. S., B. C. W. and C. A. V. were supported by CONACYT MSc scholarship.

Conflict of interest

None.

References

Ally A, Park G (1992). Rapid determination of creatine, phosphocreatine, purine bases and nucleotides (ATP, ADP, AMP, GTP, GDP) in heart biopsies by gradient ion-pair reversed-phase liquid chromatography. J Chromatogr 575: 19–27.

Balaban RS (2009). The role of Ca^{2+} signaling in the coordination of mitochondrial ATP production with cardiac work. Biochim Biophys Acta 1787: 1334–1341.

Baughman JM, Perocchi F, Girgis HS, Plovanich M, Belcher-Timme CA, Sancak Y *et al*. (2011). Integrative genomics identifies MCU as an essential component of the mitochondrial calcium uniporter. Nature 476: 341–345.

Bell CJ, Bright NA, Rutter GA, Griffiths EJ (2006). ATP regulation in adult rat cardiomyocytes: time-resolved decoding of rapid mitochondrial calcium spiking imaged with targeted photoproteins. J Biol Chem 281: 28058–28067.

Belmonte S, Morad M (2008). 'Pressure-flow'-triggered intracellular Ca^{2+} transients in rat cardiac myocytes: possible mechanisms and role of mitochondria. J Physiol 586: 1379–1397.

Benkusky NA, Weber CS, Scherman JA, Farrell EF, Hacker TA, John MC *et al*. (2007). Intact β-adrenergic response and unmodified progression toward heart failure in mice with genetic ablation of a major protein kinase A phosphorylation site in the cardiac ryanodine receptor. Circ Res 101: 819–829.

Braunwald E, Bristow MR (2000). Congestive heart failure: fifty years of progress. Circulation 102: IV14–IV23.

Brunton VG, Grant MH, Wallace HM (1990). Spermine toxicity and glutathione depletion in BHK-21/C13 cells. Biochem Pharmacol 40: 1893–1900.

Correa F, Soto V, Zazueta C (2007). Mitochondrial permeability transition relevance for apoptotic triggering in the post-ischemic heart. Int J Biochem Cell Biol 39: 787–798.

De Stefani D, Raffaello A, Teardo E, Szabò I, Rizzuto R (2011). A forty-kilodalton protein of the inner membrane is the mitochondrial calcium uniporter. Nature 476: 336–340.

Drago I, De Stefani D, Rizzuto R, Pozzan T (2012). Mitochondrial Ca^{2+} uptake contributes to buffering cytoplasmic Ca^{2+} peaks in cardiomyocytes. Proc Natl Acad Sci USA 109: 12986–12991.

García-Rivas G, Carvajal K, Correa F, Zazueta C (2006). Ru_{360}, a specific mitochondrial calcium uptake inhibitor, improves cardiac post-ischaemic functional recovery in rats *in vivo*. Br J Pharmacol 149: 829–837.

García-Rivas G, Guerrero-Hernández A, Guerrero-Serna G, Rodríguez-Zavala JS, Zazueta C (2005). Inhibition of the mitochondrial calcium uniporter by the oxo-bridged dinuclear ruthenium amine complex (Ru360) prevents from irreversible injury in postischemic rat heart. FEBS J 272: 3477–3488.

Gunter TE, Pfeiffer DR (1990). Mechanisms by which mitochondria transport calcium. Am J Physiol 258: C755–C786.

Halestrap AP (1987). The regulation of the oxidation of fatty acids and other substrates in rat heart mitochondria by changes in the matrix volume induced by osmotic strength, valinomycin and Ca^{2}. Biochem J 244: 159–164.

Jo H, Noma A, Matsuoka S (2006). Calcium-mediated coupling between mitochondrial substrate dehydrogenation and cardiac workload in single guinea-pig ventricular myocytes. J Mol Cell Cardiol 40: 394–404.

Joiner ML, Koval OM, Li J, He BJ, Allamargot C, Gazo Z *et al*. (2012). CaMKII determines mitochondrial stress responses in heart. Nature 491: 269–273.

Katz LA, Swain JA, Portman MA, Balaban RS (1989). Relation between phosphate metabolites and oxygen consumption of heart *in vivo*. Am J Physiol 256: H265–H274.

Kilkenny C, Browne W, Cuthill IC, Emerson M, Altman DG (2010). NC3Rs Reporting Guidelines Working Group. Br J Pharmacol 160: 1577–1579.

Kohlhaas M, Liu T, Knopp A, Zeller T, Ong MF, Böhm M *et al*. (2010). Elevated cytosolic Na^{+} increases mitochondrial formation of reactive oxygen species in failing cardiac myocytes. Circulation 121: 1606–1613.

Lakatta EG, Maltsev VA, Vinogradova TM (2010). A coupled SYSTEM of intracellular Ca^{2+} clocks and surface membrane voltage clocks controls the timekeeping mechanism of the heart's pacemaker. Circ Res 106: 659–73.

Lee NK, MacLean HE (2011). Polyamines, androgens, and skeletal muscle hypertrophy. J Cell Physiol 226: 1453–1460.

Lin L, Sharma VK, Sheu SS (2007). Mechanisms of reduced mitochondrial Ca^{2+} accumulation in failing hamster heart. Pflugers Arch 454: 395–402.

Liu T, O'Rourke B (2008). Enhancing mitochondrial Ca^{2+} uptake in myocytes from failing hearts restores energy supply and demand matching. Circ Res 103: 279–288.

Maack C, O'Rourke B (2007). Excitation-contraction coupling and mitochondrial energetics. Basic Res Cardiol 102: 369–392.

Maack C, Cortassa S, Aon MA, Ganesan AN, Liu T, O'Rourke B (2006). Elevated cytosolic Na^{+} decreases mitochondrial Ca^{2+} uptake during excitation-contraction coupling and impairs energetic adaptation in cardiac myocytes. Circ Res 99: 172–182.

MacDonnell SM, García-Rivas G, Scherman JA, Kubo H, Chen X, Valdivia H *et al*. (2008). Adrenergic regulation of cardiac contractility does not involve phosphorylation of the cardiac ryanodine receptor at serine 2808. Circ Res 102: e65–e72.

Mallilankaraman K, Cárdenas C, Doonan PJ, Chandramoorthy HC, Irrinki KM, Golenár T *et al*. (2012). MCUR1 is an essential component of mitochondrial Ca^{2+} uptake that regulates cellular metabolism. Nature 14: 1336–1343.

Matlib MA, Zhou Z, Knight S, Ahmed S, Choi KM, Krause-Bauer J *et al*. (1998). Oxygen-bridged dinuclear ruthenium amine complex specifically inhibits Ca^{2+} uptake into mitochondria *in vitro* and *in situ* in single cardiac myocytes. J Biol Chem 273: 10223–10231.

McCormack JG, Halestrap AP, Denton RM (1990). Role of calcium ions in regulation of mammalian intramitochondrial metabolism. Physiol Rev 70: 391–425.

McGrath J, Drummond G, Kilkenny C, Wainwright C (2010). Guidelines for reporting experiments involving animals: the ARRIVE guidelines. Br J Pharmacol 160: 1573–1576.

Michels G, Khan IF, Endres-Becker J, Rottlaender D, Herzig S, Ruhparwar A *et al*. (2009). Regulation of the human cardiac mitochondrial Ca^{2+} uptake by 2 different voltage-gated Ca^{2+} channels. Circulation 119: 2435–2443.

Neubauer S (2007). The failing heart – an engine out of fuel. N Engl J Med 356: 1140–1151.

O'Rourke B, Blatter LA (2009). Mitochondrial Ca^{2+} uptake: tortoise or hare? J Mol Cell Cardiol 46: 767–774.

Pan X, Liu J, Nguyen T, Liu C, Sun J, Teng Y *et al*. (2013). The physiological role of mitochondrial calcium revealed by mice lacking the mitochondrial calcium uniporter. Nat Cell Biol 15: 1464–1472.

Pepe S, Tsuchiya N, Lakatta EG, Hansford RG (1999). PUFA and aging modulate cardiac mitochondrial membrane lipid composition and Ca^{2+} activation of PDH. Am J Physiol 276: H149–H158.

Perocchi F, Gohil VM, Girgis HS, Bao XR, McCombs JE, Palmer AE *et al*. (2010). MICU1 encodes a mitochondrial EF hand protein required for Ca^{2+} uptake. Nature 467: 291–296.

Poburko D, Santo-Domingo J, Demaurex N (2011). Dynamic regulation of the mitochondrial proton gradient during cytosolic calcium elevations. J Biol Chem 286: 11672–11684.

Portman MA, Heineman FW, Balaban RS (1989). Developmental changes in the relation between phosphate metabolites and oxygen consumption in the sheep heart *in vivo*. J Clin Invest 83: 456–464.

Raffaello A, De Stefani D, Sabbadin D, Teardo E, Merli G, Picard A *et al*. (2013). The mitochondrial calcium uniporter is a multimer that can include a dominant-negative pore-forming subunit. EMBO J 32: 2362–2376.

Ragone MI, Consolini AE (2009). Cardiac role of the mitochondrial Ca^{2+} transporters in the high-$[K^+]$(o) cardioprotection of rat hearts under ischemia and reperfusion: a mechano-energetic study. J Cardiovasc Pharmacol 54: 213–222.

Sancak Y, Markhard AL, Kitami T, Kovács-Bogdán E, Kamer KJ, Udeshi ND *et al*. (2013). EMRE is an essential component of the mitochondrial calcium uniporter complex. Science 342: 1379–1382.

Shintani-Ishida K, Inui M, Yoshida KI (2012). Ischemia–reperfusion induces myocardial infarction through mitochondrial Ca^{2+} overload. J Mol Cell Cardiol 53: 233–239.

Silva-Platas C, García N, Fernández-Sada E, Dávila D, Hernández-Brenes C, Rodríguez D *et al*. (2012). Cardiotoxicity of acetogenins from *Persea americana* occurs through the mitochondrial permeability transition pore and caspase-dependent apoptosis pathways. J Bioenerg Biomembr 44: 461–471.

Sullivan PG, Balke CW, Esser KA (2006). Mitochondrial buffering of calcium in the heart: potential mechanism for linking cyclic energetic cost with energy supply? Circ Res 99: 109–110.

Sun Y, Zhang Y, Yan M, Wu Y, Zheng X (2009). B-type natriuretic peptide-induced cardioprotection against reperfusion is associated with attenuation of mitochondrial permeability transition. Biol Pharm Bull 32: 1545–1551.

Territo PR, Mootha VK, French SA, Balaban RS (2000). Ca^{2+} activation of heart mitochondrial oxidative phosphorylation: role of the F(0)/F(1)-ATPase. Am J Physiol Cell Physiol 278: C423–C435.

Valverde CA, Mundiña-Weilenmann C, Reyes M, Kranias EG, Escobar AL, Mattiazzi A (2006). Phospholamban phosphorylation sites enhance the recovery of intracellular Ca^{2+} after perfusion arrest in isolated, perfused mouse heart. Cardiovasc Res 70: 335–345.

Yaniv Y, Juhaszova M, Lyashkov AE, Spurgeon HA, Sollott SJ *et al*. (2011). Ca^{2+} regulated-cAMP/PKA signaling in cardiac pacemaker cells links ATP supply to demand. J Mol Cell Cardiol 51: 740–748.

Yaniv Y, Spurgeon HA, Lyashkov AE, Yang D, Ziman BD, Maltsev VA *et al*. (2012). Crosstalk between mitochondrial and sarcoplasmic reticulum Ca^{2+} cycling modulates cardiac pacemaker cell automaticity. PLoS ONE 7: e37582.

Ying WL, Emerson J, Clarke MJ, Sanadi DR (1991). Inhibition of mitochondrial calcium ion transport by an oxo-bridged dinuclear ruthenium ammine complex. Biochemistry 30: 4949–4952.

Zazueta C, Sosa-Torres ME, Correa F, Garza-Ortiz A (1999). Inhibitory properties of ruthenium amine complexes on mitochondrial calcium uptake. J Bioenerg Biomembr 31: 551–557.

Zhang SZ, Gao Q, Cao CM, Bruce IC, Xia Q (2006). Involvement of the mitochondrial calcium uniporter in cardioprotection by ischemic preconditioning. Life Sci 78: 738–745.

Zhou Z, Bers D (2002). Time course of action of antagonists of mitochondrial Ca^{2+} uptake in intact ventricular myocytes. Pflugers Arch 445: 132–138.

Supporting information

Additional Supporting Information may be found in the online version of this article at the publisher's web-site:

http://dx.doi.org/10.1111/bph.12684

Figure S1 Integrity of downstream β-adrenoceptor signalling during Ru_{360} perfusion in atrial tissue. We measured cAMP levels (panel A) and PKA activity (panel B) in atrial tissue treated with isoprenaline (ISO; 100 nM) during 10 min. We observed a significant twofold increase in cAMP and PKA activity. Panel C shows the phosphorylation of PLB-Thr^{17}. Ru_{360} treatment significantly increased PLB phosphorylation residues in response to isoprenaline, indicating that the CaMKII pathway could increase in Ru_{360}-treated atrial tissue, causing a positive chronotropic effect.